ELSEVIER

Journal of Power Sources 74 (1998) 1–7

JOURNAL OF POWER SOURCES

Dilatometry studies of phosphotungstic acid pellets during hydration and dehydration processes and design of a room temperature fuel cell

Felix B. Dias *, Julio B. Fernandes

Department of Chemistry, Goa University, Taleigao Plateau, Bambolim, Goa, India

Received 26 June 1997; accepted 9 December 1997

Abstract

Phosphotungstic acid (PWA) is still a potential solid electrolyte for fuel cells due to its high conductivity at room temperature. In this work, PWA was synthesised and characterised by X-ray, IR spectroscopy and thermal analysis. Proton number was determined by potentiometry. Characterization results agreed with those already published. Water of crystallization was determined by weight loss method on heating to anhydrous form. Changes in pellet thickness and diameter were measured as a function of water of crystallization and time for dehydration/hydration processes in controlled humid atmospheres. Geometric change parameter $\Delta L/L$, where ΔL is the change in the volume (either thickness or diameter, and L is the initial dimension) was determined for each sample. After an initial hydration or dehydration process, pellets were subsequently dehydrated or hydrated in order to study the reversibility of the geometric changes. Effects of presence of polytetrafluoroethylene (PTFE) as a binder, pelletizing pressure and particle size of PWA powder are discussed. It was found that changes in pellet diameter were greater than the pellet thickness irrespective of the pelletizing pressure and particle size. Changes in pellet thickness were lower for pellets made with higher pelletizing pressure and greater particle size, whereas changes in the pellet diameter were almost identical. The presence of PTFE lowered both the dimensional changes and the rate at which water of crystallization was lost. Interestingly, steps in the changes in pellet thickness during hydration and dehydration were observed in line with the loss of water of crystallization. Possibility of pinhole generation in the dehydrated pellets was also observed. A new fuel cell was designed, which eliminated the need of sealing the electrolyte completely in the cell. The hydrogen and oxygen gases were prehumidified to 87% relative humidities, and there was no accumulation of water at the cathode side of the fuel cell. An open circuit potential of ~ 0.7 V was observed for about 40 h during the testing of this cell. Further testing and use of this design incorporating PWA and other hydrated forms of proton conductors such as polymer membranes is suggested.

Keywords: Proton conductors; Phosphotungstic acid; Heteropolyacids; Dilatometry; Fuel cells; Fuel cell design

1. Introduction

High-energy and high-power density fuel cells are vitally needed both for terrestrial and extraterrestrial applications to minimise fuel consumption, weight, volume and capital cost of power plants [1]. Proton conductors carry charge by proton or protonic entities, and are therefore useful materials in fuel cell applications. Belonging to the group of heteropolyacids, phosphotungstic acid ($PWA \cdot 29H_2O$) has been much investigated as a solid electrolyte for room temperature H_2/O_2 fuel cells because of its 29 hydrated form showing exceptionally large proton conductivities of 0.18 S cm^{-1} at 20°C [2–6]. Prehumidification of the fuel gases in order to maintain the high hydration level in the solid electrolyte is necessary [3]. Thus, $PWA \cdot 29H_2O$ requires a relative humidity (r.h.) of about 90% for its stability [7]. PWA has a high tendency to dissolve at the oxygen electrode surface during the fuel cell operation, and this can cause serious problems with large amounts of water formed at the cathode during the fuel cell operation. Use of polytetrafluoroethylene (PTFE) in the PWA has been found, to some extent, to reduce this tendency, apart from acting as a binder for mechanically stable pellets to be formed [8]. Use of 30% by weight of PTFE in PWA was found to be optimum, and could also retain the high conductivity of PWA in the composite [8]. Interest in the testing of the phosphotungstic acid in low temperature fuel cells still continues [5,6]. Giordano et al. found an output

* Corresponding author. Department of Engineering Materials, University of Sheffield, Mappin Street, Sir Robert Hadfield Building, Sheffield S1 4DU, UK.

0378-7753/98/$19.00

power of 700 mW cm^{-1} at 25°C with life times of more than 300 h [6]. Earlier, Nakamura et al. had reported an electromotive force of 0.8 V and a maximum current density of 50 mA cm^{-1} for a cell using Cu_2O as the oxygen electrode [3].

In order to form mechanically stable pellets for use in fuel cells, large pelletizing pressures have to be applied. In the case of phosphotungstic acid, since large amount of water of crystallization is required to maintain its high conductivity at room temperature, large pressures may be unfavourable. Water of crystallization has been found to be lost even when pressures of about 1000 kg cm^{-2} were applied during pelletization, thereby decreasing their conductivities below acceptable values. Thus, Nakamura et al. used humid atmospheres during crushing of the crystals and during pelletization [9]. Giordano et al. mixed PTFE to the phosphotungstic acid powder that acted as a hydrophobic material and reduced the dissolution of the solid electrolyte pellet by the water formed during the fuel cell reaction [8].

Fuel cell assemblies using solid electrolytes require the solid electrolyte pellets to be sealed between fuel cell gas compartments, thereby acting as gas barriers preventing intermixing of the fuel cell gases. Due to possible variations in humidities and operational temperatures in the fuel cell, phosphotungstic acid pellets can undergo reversible hydration–dehydration reactions accompanied by reversible or irreversible changes in their geometric configurations. Also, dehydration can result in the formation of tiny holes in the solid electrolyte. The work reported in this paper aroused interest when in one of the fuel cells designed, we found that the solid electrolyte pellet did not fit in the fuel cell configuration after a couple of days in open atmosphere, although all dimensions were correct when the solid electrolyte pellet was freshly made. Therefore, we have investigated the changes in the pellet geometry in presence of varying humid atmospheres. Effects of pelletizing pressures and the presence of PTFE as a binder are also discussed. We also made a new design of a fuel cell that allowed the pellet to freely change dimensions during the fuel cell operation. The OC characteristics of this cell are reported.

2. Experimental

2.1. Synthesis and characterization

The phosphotungstic acid ($H_3PW_{12}O_{40} \cdot xH_2O$) was synthesised using Bailer's procedure [10], which involved the addition of $NaHPO_4$ to boiling $NaWO_4$ solution in the presence of conc. HCl, followed by ether extraction and crystallization. The powder was redissolved in water and subjected to slow crystallization at room temperature. The hexagonal crystals thus obtained were crushed, ground to fine powder, and stored over saturated KCl solution till constant weight was attained.

Chemical composition of the synthesised PWA was confirmed as follows. The tungsten:phosphorous ratio as determined by chemical analysis [11] was found to be 12.01:1.0. The number of replaceable hydrogens were determined potentiometrically using 0.05 M NaOH as the titration base [12]. All solutions for the potentiometry were made in aquaeous 40% 1,3-dioxane solvent. From the titration curve, pH vs. moles of NaOH added per mole of the acid, a proton number of 3.0 was obtained corresponding to 3.0 mol of NaOH per mol of acid. Complete decomposition of the acid corresponded to 26.0 mol of NaOH per mol of acid in accordance with the literature [12]. Water content per formula unit was calculated from weight loss upon heating the acid to its anhydrous form at 300°C for about 1 h [13]. Differential thermal analysis was carried out in a nitrogen atmosphere on a VEB Ultraschallteknik, Germany DTA instrument, using α-Al_2O_3 as a reference standard, with a heating rate of 5°C m^{-1}. XRD spectrum was taken on a JOEL, JDX-8P X-ray diffractometer using CuKα radiation. Table 1 gives the characterization values for the phosphotungstic acid in comparison with the published results, which are in agreement with each other. An atmosphere of 87% relative humidity was provided to the sample during the XRD run by passing air from an air pump through a series of saturated KCl solutions. The sample was found to have $n = 21$ as water of crystallization, which was determined as explained above. Infrared spectrum was recorded in the range 6000–400 cm^{-1} in a KBr pellet using 'Pyeunicam' infrared spectrometer. Dimensions of pellets were measured using a micrometer gauge with an accuracy of ± 0.005 mm. A glossy paper was used to cover the surfaces of the pellets during the measurement in order to prevent loss of the surface material due to probe friction, and also to avoid contact of metal to the PWA pellets. Measurements were corrected for the presence of this glossy paper. Geometric change parameter $\Delta L/L$, where ΔL is the change in the geometry (either thickness or diameter), and L is the initial dimension, was determined for each sample. Hydration and dehydration of pellets were performed in dessicators equilibrated with saturated solutions of $NaHCO_3$ ($\sim$95% r.h.) and $NaNO_3$ ($\sim$82% r.h.) respectively. A reference pellet was also treated similar to the experimental sample for determination of water of crystallization. Relative humidities (r.h.) during various stages of this investigation were determined using a Barigo (Germany) thermohygrometer.

2.1.1. PWA pellets

$PWA \cdot 21H_2O$ was pelletised at pressures of 7 and 8 kg cm^{-2} using a Teflon die to form pellets of diameter 12.8 mm. About 2.64–2.90 mm thick pellets were obtained depending on the pressure and the amount of sample. Although no water of crystallization was found to lose during pelletization, the pellets were ensured of their initial 21-hydrate by maintaining them over saturated KCl solu-

Table 1
Characterization of $H_3PW_{12}O_{40} \cdot xH_2O$ by DTA, XRD, and IR spectroscopy

DTA (°C)		X-ray diffraction				IR spectroscopy (cm^{-1})	
Observed	Refs. [14,15]	Observed		PDF data No. 38077		Observed	Ref. [14]
		% Relative intensity	*d*-values (Å)	% Relative intensity	*d*-values (Å)		
Endotherms 110, 210	Endotherms 110, 212	100	8.191	100	8.197	1080	1080
Exotherms 568, 615	Exotherms 560, 615	100	3.376	100	3.344	982	983
		100	2.931	100	2.907	890	890
		100	2.484	100	2.481	805	809
		81	5.791	80	5.814		
		100	4.133	80	4.115		
		78	2.262	80	2.278		
		43	4.796	60	4.739		
		46	3.685	60	3.676		
		39	2.779	30	2.740		
		39	2.528	20	2.597		
		16	6.711	10	2.711		

Comparison of observed and literature values.

tion, till constant weight was attained. Pellets with approximately three times particle size than the above were also prepared using PWA powder passed through nylon sieves of definite mesh size. Average particle size of the powdered PWA was measured approximately using an Olympus transmission light microscope.

2.1.2. Solid-electrolyte / PTFE composite

About 2 g of $PWA \cdot 21H_2O$ was mixed with 30% by weight of PTFE (emulsion Fluon GP2) using cyclohexane as the dispersion medium in an ultasonicator. The mixture was then dried in a dessicator containing saturated KCl at room temperature for minimum 24 h till constant weight was attained. The mixture was finally pressed at 7 kg cm^{-2} using a Teflon die to form a 12.8 mm pellet. Using ~ 0.2 g of $PWA \cdot 21H_2O$ and 30% by weight PTFE emulsion, a 1.2 mm thick and 12.8 mm o.d. composite pellet was obtained, which was used in the fuel cell testing.

2.1.3. Electrodes

Sheets of porous electrodes were supplied by BHEL, Hyderabad (India). A sheet consisted of an outer layer (0.15 mm i.t.) made of 10% Pt by weight dispersed on active carbon and an inner layer (0.35 mm i.t.) made of graphite-PTFE mixture (Fig. 6). Circular electrodes of the required dimensions were then cut out.

3. Results and discussion

3.1. Dilatometry studies

Fig. 1 shows changes in the pellet thickness for dehydration and hydration processes for pellets with and without PTFE content. As can be seen, for pellets without PTFE, changes in pellet thickness for both dehydration and hydration processes were almost the same. Also, subsequent dehydration and hydration after the pellets had undergone initial hydration and dehydration, respectively, did not show much difference in the rates of change of pellet thickness. Changes in pellet thickness for the pellet containing 30% PTFE binder during hydration were slower than those without the PTFE. In Fig. 1, a sudden fall in the pellet thickness after ~ 20 h for the pellet containing PTFE can also be seen. It was earlier observed that PTFE free pellets became softer as water of crystallization reached $n = 30$. Thus, the softening would lead to the measurement

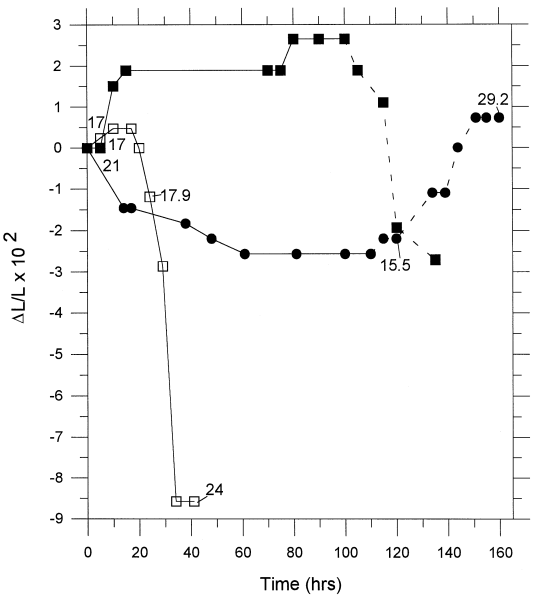

Fig. 1. Changes in pellet thickness with time. Dehydration from $n = 21$ to 15.5 (● ————) and subsequent hydration (●- - -). Hydration from $n = 17$ to 29 (■ ————) and subsequent dehydration (■- - -). Hydration of pellet containing 30% PTFE, from $n = 17$ to 24 (□ ————).

probe compressing the pellet and reducing the measurable thickness.

From Fig. 2, we can see that during the hydration processes, changes in pellet diameter were greater than those of pellet thickness, more or less irrespective of pelletizing pressures and particle size of the powder used in the pelletization. Nevertheless, lower changes in pellet diameter for pellet pelletised at 11 kg cm^{-2} than the one pelletised at 7 kg cm^{-2} can be seen. Also the changes in pellet thickness during the initial hydration processes were smaller for the pellet with higher pelletizing pressure. The pellet with about three times higher particle size also lowered changes in both the diameter and the thickness of the pellet during the hydration processes.

However, for subsequent dehydration processes, the following observations can be made from the plots in Fig. 2. For the pellet pelletised at 7 kg cm^{-2}, the changes in the pellet thickness were greater than those of the pellet diameter, whereas at 11 kg cm^{-2}, they were almost the same. The changes in pellet thickness for pellet pelletised at 11 kg cm^{-2} were slower than those at 7 kg cm^{-2}, indicating greater compaction of particles reducing the geometric change; whereas this effect was negligible in the changes of the pellet diameter. The figure also shows that the 3 × particle size of pellet powder does not have much

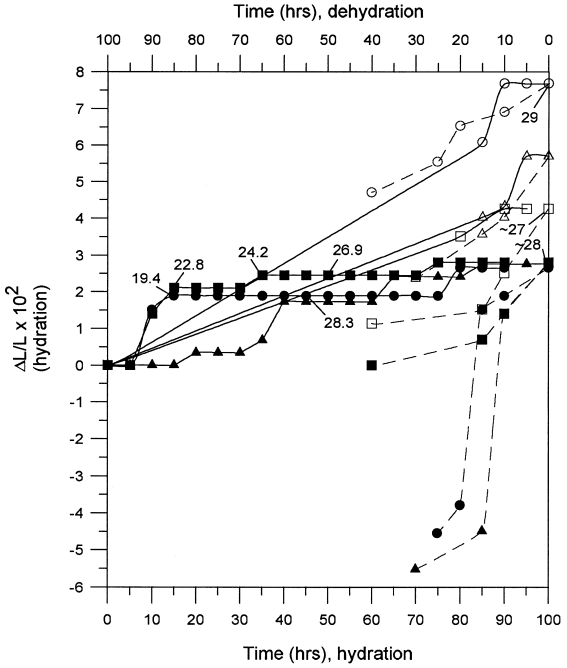

Fig. 2. Simultaneous changes in pellet thickness and pellet diameter on hydration and subsequent dehydration, effects of pelletizing pressure and particle size. Changes in pellet thickness: 7 kg cm^{-2}, hydration (● ————), subsequent dehydration (●- - -); 11 kg cm^{-2}, hydration (■ ————), subsequent dehydration (■- - -); particle size = ~3×, hydration (▲ ————), subsequent dehydration (▲- - -); Changes in pellet diameter: 7 kg cm^{-2}, hydration (○ ————), subsequent dehydration (○- - -); 11 kg cm^{-2}, hydration (□ ————), subsequent dehydration (□- - -); particle size = ~3×, hydration (△ ————), subsequent dehydration (△- - -).

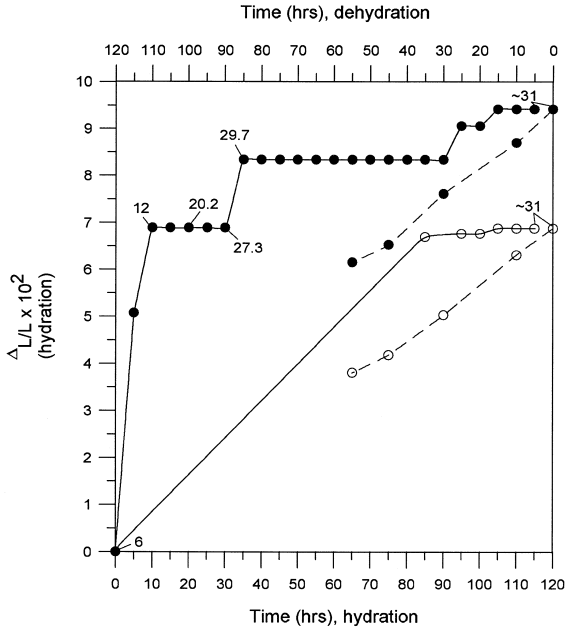

Fig. 3. Simultaneous changes in thickness and diameter on hydration and subsequent dehydration for pellets heated to 120°C. Changes in pellet thickness, hydration (● ————), subsequent dehydration (●- - -). Changes in pellet diameter, hydration (○ ————), subsequent dehydration (○- - -).

effect on the change of both pellet thickness and diameter at the same pelletizing pressure, since the changes are almost identical.

An interesting observation in the Fig. 2 is the steps in which the pellet thickness changes as the pellets were hydrated with time, although in some cases measurements could not be made between 0 and 80 h. At the same pelletizing pressure, steps can be observed at about the same time of hydration for the pellets of different particle size. For the pellet pressed at 7 kg cm^{-2}, a step at ~30 h of hydration can be observed, which is not seen in pellet pressed at 11 kg cm^{-2}. Also, changes in both the pellet thickness and diameter during the subsequent dehydration of all samples slowed down after about 10 min of dehydration time. This may well correspond to the degree of hydration in the samples (corresponding to the hydration phases in PWA reported by Nakamura et al. [7]) since they were all initially hydrated roughly to the same level (n = 27–29). In Fig. 2, during the initial hydration process, leveling of pellet thickness with time can be observed for the pellets pressed at 7 and 11 kg cm^{-2} having the same particle size, whereas, the one with greater particle size lagged behind the other two at the same pelletizing pressure of 7 kg cm^{-2}. Observations under an optical microscope after the leveling time showed that the particles in the pellet pressed at 7 kg cm^{-2} were larger than those in the pellet pressed at 11 kg cm^{-2}, and also larger than the original size before the hydration process. Unfortunately, no optical micrographs could be taken during the experiment.

From Fig. 3, we can observe greater changes in the pellet thickness than the pellet diameter during hydration up to $n = \sim 29$ in contrast with observations in the Fig. 2. This difference could be due to the fact that the pellet in Fig. 3 was dehydrated by heating at 120°C to $n = 6$, whereas that in Fig. 2 was dehydrated in low humidity atmosphere to $n = 17$ prior to the hydration experiments. This would explain greater particle compaction along the thickness of the pellet, which has more water of hydration (sort of a inter-particle fusion aided by the water molecules). In the Fig. 2, the subsequent dehydration processes are rapid, and changes in pellet thickness and diameter are almost identical. Along with Fig. 2, Fig. 3 shows irreversibility in the initial hydration and subsequent dehydration processes, indicating the possibility of pinhole generation in the pellets, which would further affect their function as gas barriers between hydrogen and oxygen gases during the fuel cell operation. The figures also show that only during the initial hydration or dehydration processes that differences in pellet thickness and diameter can be seen, and changes in pellet thickness and diameter after the initial processes are almost the same.

Changes in water of crystallization (n) in the pellets during hydration and subsequent dehydration are shown in Fig. 4; whereas, Fig. 5 shows the reverse in which the pellet was initially dehydrated and subsequently hydrated. As can be seen from the Fig. 4, water of crystallization in the hydrated pellets is lost more rapidly compared with the rate at which it would gain during an initial hydration process. Pellet pressed at 11 kg cm^{-2} lost water of crystallization at a lower rate than the one pressed at 7 kg cm^{-2}, the latter possibly having a greater surface area for absorption of water on its surface and in the bulk. The presence of 30% PTFE in the pellet lowered the rate at which the water of crystallization was gained during hydration of the pellets. Fig. 5 indicates that the initial dehydration of the pellet was slower than its subsequent hydration (seen as a hysterisis loop in the figure). Thus, it can be said that the rate of crystallization would depend on the hydration state at which the pellet is initially made; the initial processes only changing the compactness of the pellet particles, which is not reversible during subsequent crystallization processes. In a separate observation, the dehydrated pellet was found to have loose particles on its surface, which later got adhered to neighbouring particles when the pellet was subsequently hydrated. This probably would indicate the possibility of shrinking of particles in the pellet, leaving tiny spaces or pinholes during dehydration, in line with previous observations and discussed in the preceding paragraphs. Due to the presence of these spaces, subsequent hydration processes seem to be easy, and hence take place at a faster rate as already discussed (Fig. 5).

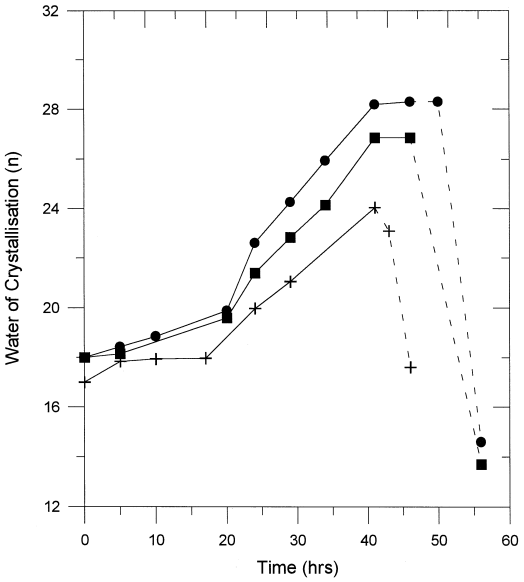

Fig. 4. Water of crystallization vs. time for pellets hydrated (from $n = 17$) and subsequently dehydrated, effects of pelletizing pressures and presence of PTFE binder. 7 kg cm^{-2}, hydration (● ————) and subsequent dehydration (●- - -); hydration (■ ————) and subsequent dehydration (■- - -); 7 kg cm^{-2}, hydration of pellet containing 30% PTFE (+ ————), subsequent dehydration (+- - -).

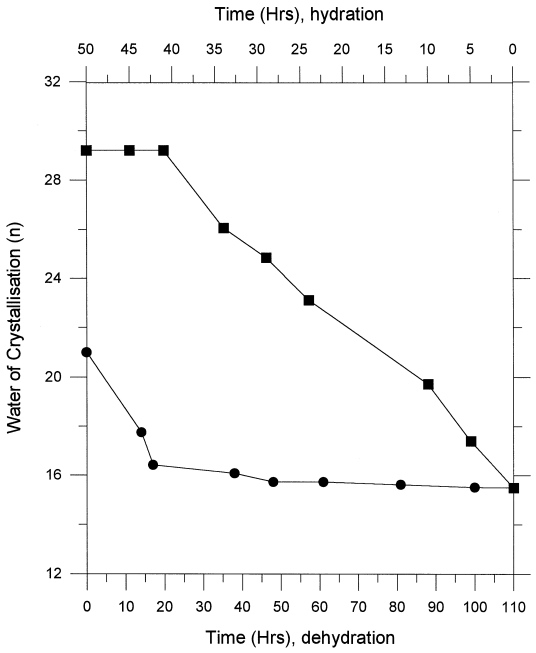

Fig. 5. Water of crystallization vs. time for dehydration (●) and subsequent hydration (■) processes.

3.2. Fuel cell studies

We found that at pelletizing pressure of 7 kg cm^{-2}, there was no loss of water of crystallization from the PWA pellet as measured by the weight loss method [13]. We observed that when PWA alone was pelletised at a pressure of 1000 kg cm^{-2}, there was loss of water of crystallization even at an atmosphere of 90% relative humidity, contrary to literature reports [4].

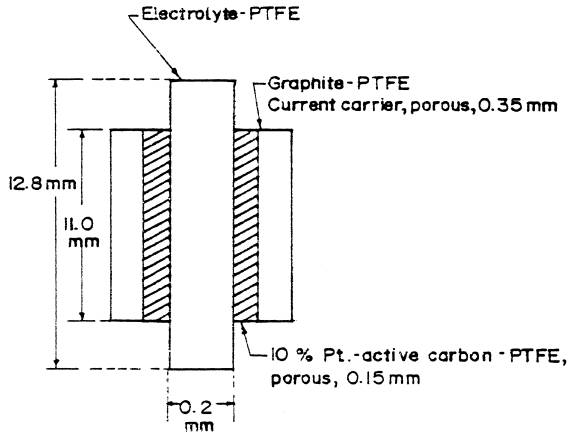

Fig. 6. Electrode/electrolyte/PTFE composite showing relative dimensions.

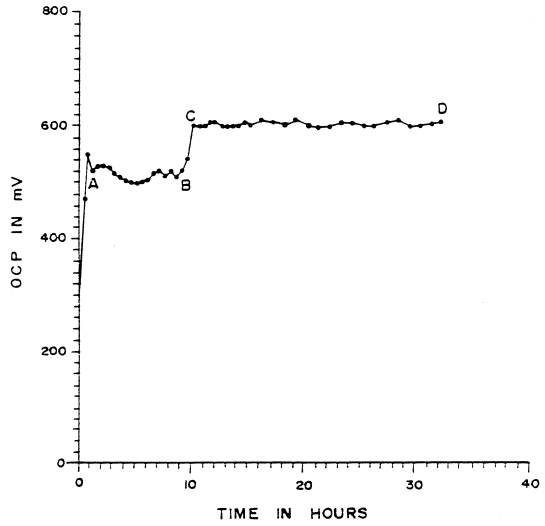

Fig. 8. Open circuit potential vs. time characteristics for the fuel cell H_2/PW A.21-29H_2O-PTFE/O_2.

Fig. 6 gives a schematic representation of the electrode/solid electrolyte composite. It can be seen that the diameter of the solid electrolyte composite is *greater* than that of the facing electrodes. Fig. 7 schematically shows the actual fuel cell assembly. The electrode/electrolyte composite was well secured between two platinum meshes with sport-welded platinum leads. During the fuel cell operation, the electrodes were continuously bathed (at nearly zero pressures) with prehumidified H_2 and O_2 gases (87% relative humidity). It may be noted that in this cell design, there were no outlets for the unreacted gases; the fuel gases were merely in contact with the electrode surface, thus economizing the use of the fuel cell gases. The electrolyte, which was partially open at its continuous circular edges (see Fig. 1), was maintained in a dynamic environment of pre-humidified air at 87% relative humidity.

Fig. 8 shows a typical pattern of the variation of open circuit potential of the fuel cell when the electrode–electrolyte composite was kept in continuous contact with the pre-humidified H_2 and O_2 gases at 87% relative humidity. From the figure, one can see a sudden rise in the voltage to the point 'A' during the optimization of the pressures of H_2 and O_2 fuel gases. From point 'A' to 'B', the PWA is presumably a 21 hydrate (the same before the reaction was started), which increases to 29 hydrate at point 'C'. The increase in the voltage is probably due to an increase in

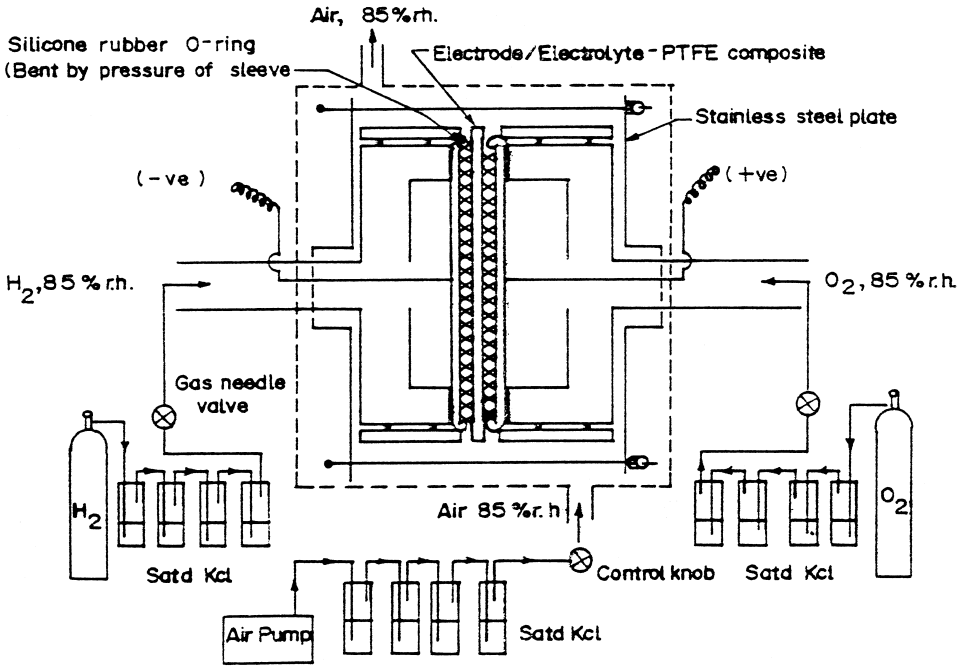

Fig. 7. Schematic representation of the H_2/solid electrolyte/O_2 fuel cell assembly.

conductivity of the PWA on the gain of the water of crystallization, as shown by Nakamura for ex situ conductivity measurements on PWA pellets [9]. The 29 hydrate is stable in the range of 90–95% relative humidity [7]. The use of PTFE allowed thin pellet fabrication, reduced the dissolution of the PWA by water, and prevented water drag from cathode to anode during the fuel cell reaction, which is in accordance with earlier observations [8]. Thus, we concluded that the continuously flowing humidified air at 85% relative humidity not only swept away the excess water from the electrolyte surface on the oxygen electrode side, but also kept the solid electrolyte stable to its 29-hydrate. In this investigation, we generally observed a constant open circuit potential of ~ 0.7 V for more than 44 h. The present design eliminated the requirement of sealing the solid electrolyte in the fuel cell compartment.

4. Conclusions

The results on the dilatometry studies are interesting when fuel cell fabrication is concerned using phosphotungstic acid as the solid electrolyte. Differences in the pellet thickness and diameter are more significant in freshly prepared pellets and during the initial hydration or dehydration process. Changes in pellet thickness and diameter after the initial processes are almost the same. Changes in the water of crystallization of the pellets depend on the initial hydration state of the pellet, and the pelletizing pressure or the compactness of the pellet particles. The higher the pelletizing pressure, the lower is the change of pellet thickness and the rate of hydration. The presence of PTFE slows down both the rates. The changes in the compactness of the particles seem to be irreversible before and after hydration or dehydration, resulting into generation of small spaces that would be disadvantages for a fuel cell operation. The reported geometric changes taking place in the pellet under various hydrated and dehydrated conditions, and the accompanying loss or gain of water of crystallization, will help in the design of fuel cells.

The new design of the fuel cell, eliminated the problem of pellet expansion in presence of varying humidity atmospheres by keeping part of the pellet exposed to an external humid atmosphere. There was no accumulation of water at the cathode and the PWA was at its 29 hydrate during the fuel cell operation. Presence of PTFE in the PWA pellet allowed very low pelletizing pressures, which prevented the loss of water of crystallization during the pelletization. Further, longer testing of the cell at zero current and under various current drains needs to be done. The design can be used in conjunction with other hydrated forms of proton conductors.

Acknowledgements

FBD would like to thank the Department of Science and Technology, Government of Goa, India for funding the project. The authors would also like to thank Prof. A.K. Shukla, I.I.Sc. Bangalore for assisting in the designing of the fuel cell.

References

[1] S. Srinivasan, O.A. Velev, A. Partasarathy, D.J. Manke, A.J. Appleby, J. Power Sources 36 (1991) 299.
[2] O. Nakamura, T. Kodama, I. Ogino, Y. Miyake, Chem. Letters (1979) 17.
[3] O. Nakamura, T. Kodama, I. Ogino, M. Adachi, U.S. Pat. 4554 224 A (19 Nov. 1985).
[4] O. Nakamura, Prog. Batt. Sol. Cells 4 (1982) 230.
[5] N. Giordano, P. Staiti, A.S. Arico, E. Passalacqua, L. Abate, S. Hocevar, Electrochim. Acta 42 (11) (1997) 1645.
[6] N. Giordano, P. Staiti, S. Hocevar, A.S. Arico, Electrochim. Acta 41 (3) (1996) 397.
[7] O. Nakamura, I. Ogino, T. Kodama, Solid State Ionics 3 (1981) 347.
[8] N. Giordano, P.L. Antonucci, S. Hocevar, Z. Pottarzewski P. Staits, Proc. Sym. Energy Technol. Abstr. No. 481, Washington DC, 1991.
[9] O. Nakamura, I. Ogino, Mater. Res. Bull. 17 (2) (1982) 231.
[10] J.C. Bailer, Inorg. Synth. 1 (1939) 132.
[11] H. Hayashi, J.B. Moffat, Talanta 29 (1982) 943.
[12] G.A. Tsigdinos, C.J. Hallada, J. Less Common. Met. 36 (1974) 73.
[13] E.M. Serwicka, K. Bruckman, J. Haber, E.A. Paukshtis, E.N. Yurchenko, Appl. Catal. 73 (2) (1991) 153.
[14] Y. Zuolong, L. Shufang, H. Furong, W. Shunli, Z. Guilin, Z. Suxian, Kexue Tongbao 32 (22) (1987) .
[15] B.K. Hodnett, J.B. Moffat, J. Catal. 88 (2) (1984) 253.